COBEM 2021 26th International Congress of Mechanical Engineering
November 22-26, 2021, Virtual Congress, Brazil
ABCM Associação Brasileira de Engenharia e Ciências Mecânicas

COB-2021-1343
TRANSMISSION LOSS OF DECORATED MEMBRANE RESONATORS PANELS USING MODAL-BASED NUMERICAL METHODS: A COMPARISON

Pedro C. M. Cerântola
Universidade de São Paulo - Escola de Engenharia de São Carlos, Av. Trabalhador Sancarlense, 400, 13565-090, São Carlos/SP, Brazil
pedro.cerantola@usp.br

Lauren Maxit
Laboratoire Vibrations Acoustique, INSA-Lyon, 25 bis av. Jean Capelle, F-69621 Villeurbanne Cedex, France
laurent.maxit@insa-lyon.fr

Leopoldo P. R. de Oliveira
Universidade de São Paulo - Escola de Engenharia de São Carlos, Av. Trabalhador Sancarlense, 400, 13565-090, São Carlos/SP, Brazil
leopro@sc.usp.br

Abstract. *The always-increasing demand for energy efficiency in vehicles and machines inevitably drives designs towards lightweight structures, posing a challenge for noise and vibration. The difficulties are even greater if passive control is needed to address the low-frequency range, which will often lead to heavy and bulky solutions. Having the capability of outperforming the mass-law of acoustics, Membrane Acoustic Metamaterials (MAM) have been recently studied in panel configurations as a potential lightweight solution for sound insulation in the low-mid frequency range. MAM are realised by a stretched membrane over a regular frame, resulting in a arrangement that tessellates the plane. Decorated Membrane Resonators (DMR) are the most commonly MAM setting employed, with a concentrated mass added to the unit cells. At the present time, most of the research made focuses on analysing the behaviour of unit cells rather than the full metastructure, mainly due to computational costs. If deeper and more practical investigations are to be exploited, methods other than the direct approach – commonly used in finite elements modelling environments – should be validated. To tackle such a challenge, this paper studies the efficiency and accuracy of two techniques for predicting the Transmission Loss (TL) of a MAM metapanel separating two acoustic cavities: the Dual Modal Formulation (DMF) and the Statistical Modal Energy Distribution Analysis (SmEdA). While the former is based on modal expansions considering the uncoupled-blocked modes for the cavities and the uncoupled-free modes for the panel, the latter consists of an extension of the well-known Statistical Energy Analysis (SEA) method that relaxes the modal energy equipartition assumption. The two approaches are based on the same subsystem modes but they differ by the resolution: DMF condensates the modal participation factors of the non-excited subsystems while SmEdA establishes the power balance equations between the subsystem modes by using a formulation for two coupled oscillators. Aside TL, a comparison is made over the computational cost associated with both methods for the solving of the vibro-acoustic problem we propose.*

Keywords: *Membrane Acoustic Metamaterials (MAM), Dual Modal Formulation (DMF), Statistical Modal Energy Analysis (SmEdA), Decorated Membrane Resonator (DMR), Transmission Loss (TL)*

1. INTRODUCTION

In the past few decades, engineers have been leaning into new techonological alternatives to develop devices at the same time energy efficient and silent (Fan *et al.*, 2015). Ruiz *et al.* (2018) and Venter *et al.* (2016) searched control strategies for industrial machines, such as lathes and robots, while Mosquera-Sánchez *et al.* (2017b,a, 2018) looked to reduce noise inside vehicles. The so-called acoustic metamaterials - structures based on periodicity or local resonances which presents abnormal properties in a specific frequency or frequency range - can be considered as a new alternative. Aside the Helmholtz resonators and the designs that rely on the Bragg's scattering phenomenon (Bragg and Bragg, 1913), Membrane Acoustic Metamaterials (MAM) are in ever-increased evidence (Chen *et al.*, 2014; Fan *et al.*, 2015).

Capable of offering high levels of Transmission Loss (TL) with very little added mass, MAM are specially efficient on insulating low frequency noise, which can defy the mass-law (Yang *et al.*, 2008). The downside of the concept is the narrow band in which this phenomenon is produced, what raises the need of MAM operated in association. In terms of final applications, this aspect can be easily surpassed, as both the automotive and aerospace industries - which have in

noise attenuation and weight reduction a very appealing necessity (Aridogan and Basdogan, 2015; Aloufi *et al.*, 2016) and, therefore, potential of MAM usage - are known to employ plate-like structures - that can, in turn, act as basis for MAM panels. In fact, this possibility is already tackled, and relevant studies have been produced, such as Langfeldt *et al.* (2018), Sampaio *et al.* (2019), Nguyen *et al.* (2021) and Ma *et al.* (2021).

From a wider overview, the research on acoustic metamaterials is currently focused on optimising their attenuating band. For MAM, this is perfectly outlined by their dynamic behaviour: each unit cell - generally a Decorated Membrane Resonator (DMR), which consists of a pre-stressed membrane with an attached concentrated mass - presents as the first two vibration modes the piston mode (0,1), in which the mass moves back and forth like a piston, and the membrane mode (0,2), in which the mass stands still and the rest of the membrane oscillates around it. According to Yang *et al.* (2008), the noise attenuation property comes from the anti-resonance in between these two modes. This dynamic is depicted in Fig. 1.

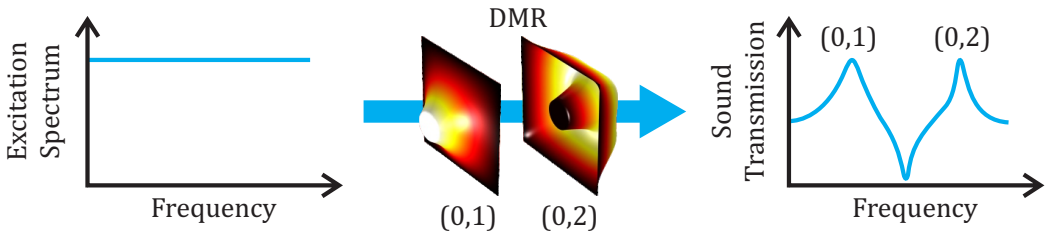

Figure 1. Sound Transmission of a DMR including membrane resonant modes (0,1) and (0,2).

Another standpoint that deserves some scientific interest when it comes to MAM is the mathematical understanding and modelling of these devices. As cavities + DMRs panels systems are complex and multifaceted, while analytical approaches are valuable - Guy (1979); Pan and Bies (1990); Hong and Kim (1995) offer details on the matter of fluid/structure interaction -, numerical techniques must be put to use if the system is to be characterised in detail. In this context, mesh-based routines are popular, and within those, Finite Elements Method (FEM) and Statistical Energy Analysis (SEA) are the most common environments for solving the sound transmission problem. The most suitable strategy is often given both by the system size and the frequency range (Martin, 2015).

For the low frequency range, deterministic techniques such as the direct method using FEM are viable and reasonable in terms of computational cost (Sandberg and Ohayon, 2009). This is true due to the reducer modal density and enhanced wavelengths, which permits the description of the system with relatively few Degrees of Freedom (DoFs). For mid or high frequency ranges, with the growth of DoFs - linked to the necessary refinement of the mesh - statistical and modal methods are more popular. This includes the Dual Modal Formulation (DMF), the well-known Statistical Energy Analysis (SEA) and, finally, the Statistical modal Energy distribution Analysis (SmEdA) (Maxit, 2013). That said, it is still of interest, primarily considering a system as complex as a MAM's panel, to diminish computational cost in the low frequency range without loosing accuracy.

This paper aims to evolve on the matter of numerical handling of acoustic metamaterials. The sound transmission through a simplified MAM panel dividing two cavities is planned to be assessed by using three different techniques: the FEM direct method, that shall be considered as reference, the DMF and the SmEdA. The text is organised as follows:

- In Section 2. the investigated system is described and presented in detail. Altogether, the proposed indicators to evaluate the vibro-acoustic performance of the panel and the quality of the algorithms applied are introduced;

- The numerical benchmark used as tool in this work is presented in Section 3. Taken as reference, the FEM model is outlined in Subsection 3.1 The modal basis produced with FEM is indicated in Subsection 3.2, and finally both the DMF and SmEdA methods are described in Subsections 3.3 and 3.4, respectively.

- Results obtained with the procedures are shown and preliminarily discussed in Section 4.

- Section 5 brings the most important observations and conclusions over the work conducted, as well as recommendations and pointings of future effort that could be made on the topic.

2. PROBLEM STATEMENT

A vibro-acoustic system with a simple geometry is investigated in order to predict the sound transmission phenomenon through a MAM metapanel. It consists of a cavity-panel-cavity arrangement, being V_1 and V_2 the volumes of the exciting and receiving cavity, respectively. A monopole sound source of unit volume velocity is positioned inside cavity V_1, and a metapanel of area S stands simply supported between V_1 and V_2. The panel consists of an assembly of three square unit cells of sides 5, 10 and 20 centimetres. In total, there are 114 cells (96 small, 16 medium and 2 large). The main

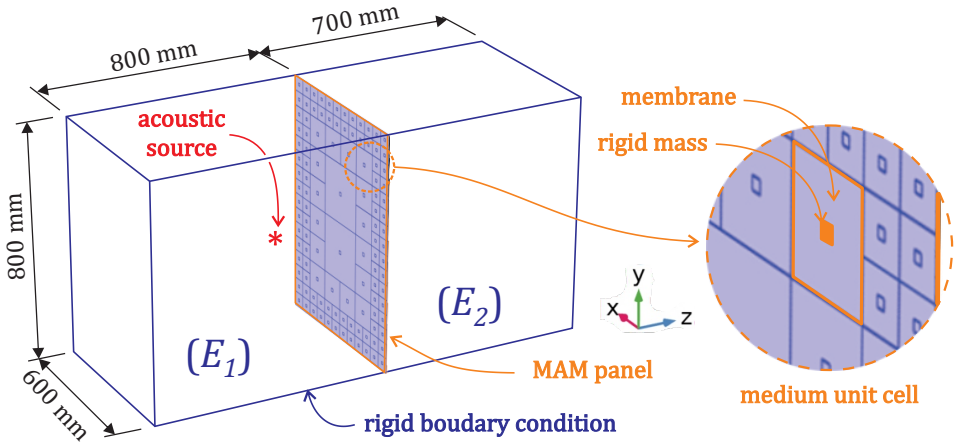

Figure 2. Sketch of the vibro-acoustic system.

Table 1. Material properties of the nominal system (panel thickness t = 1.2 mm).

Membrane	
Mass density	$\rho_{memb} = 960\ kg/m^3$
Young modulus	$E_{memb} = 8\ MPa$
Poisson's ratio	$\nu_{memb} = 0.48$
Damping loss factor	$\eta_{memb} = 0.01$
Concentrated mass	
Mass density	$\rho_{mass} = 8100\ kg/m^3$
Young modulus	$E_{mass} = 150\ GPa$
Poisson's ratio	$\nu_{mass} = 0.3$
Damping loss factor	$\eta_{mass} = 0.01$
Material: Air at STP	
Mass density	$\rho_0 = 1.29\ kg/m^3$
Speed of sound	$c_0 = 340\ m/s$
Damping loss factor	$\eta_0 = 0.01$

parameters of the panel and the cavities are given in Tab. 1, while the assembly and measures of the system can be seen in Fig. 2.

The source is placed at $(x, y, z) = (0.24, 0.42, 0.54)\ m$ - close to the panel in the emitting cavity V_1. The monopole provides a white noise of constant spectrum $S_{Q_0Q_0}$, which disturbs the panel. This perturbation is transmitted via the panel to the cavity V_2, making it possible to evaluate the sound insulation provided by the metastructure. Multiple indicators can be utilised to characterise the insulation properties of structures, such as the Sound Reduction Index (SRI), the Insertion Loss (IL) and the Transmission Loss (TL) (Möser and Zimmermann, 2004). While both SRI and IL depend on the external conditions of the test, TL is a function of the investigated structure only. For this reason, TL will be used as main metric in the present work.

The design of the metapanel deserves some attention here. Devices based on local resonances present attenuation only in a narrow frequency band (Yang *et al.*, 2008; Sampaio *et al.*, 2019). The periodicity and variability of unit cells are desirable to open a TL gap, which, in addition to the need of the system to attenuate multiple regions inside a third-octave for the SmEdA and DMF methods to properly identify the action of the panel over the average TL, leads to the concept of unit cells with different configurations for the panel.

Cells properties can be seen in Tab. 2, while the frequency response profile of the cells is observed in Fig. 3. Notice that all three TLs peak at the 15^{th} third-octave of the spectrum, between 447 and 562 Hz - which is the aimed region to attenuate with the proposed metapanel.

Table 2. Parameters of the three designed square metapanel cells.

	Large	**Medium**	**Small**
Side	20 cm	10 cm	5 cm
Pre-stress	9 MPa	5 MPa	2 MPa
Concentrated mass	3 g	3 g	2 g

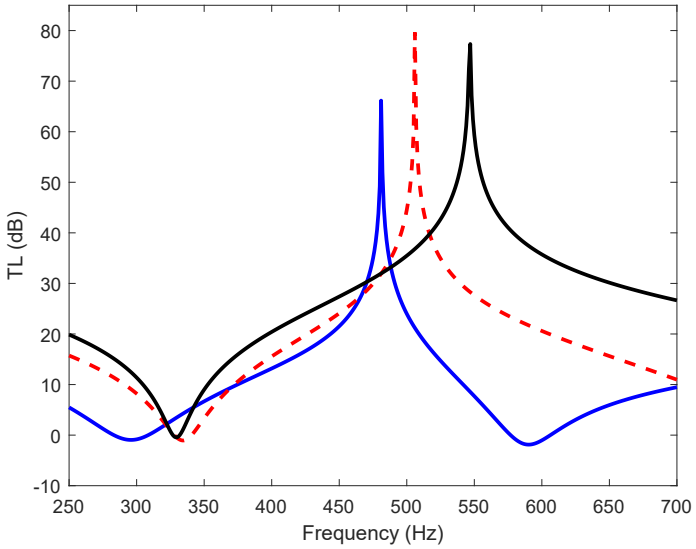

Figure 3. TL peaks of the three different designed metapanel cells. Blue solid line, large; red dashed line, medium; black solid line, small.

3. NUMERICAL BENCHMARK

3.1 Reference: FEM - Direct Method

At first, the harmonic response of the vibro-acoustic dynamic system is obtained through a FEM model with the software COMSOL Multiphysics. The simulation consisted on the application of both a simple modal analysis conducted to the panel - that functioned as input to the modal-based techniques applied afterwards - and the direct method - the solving of the dynamic system for the Helmholtz equation coupled with the Newton-Euler equation - from 355 to 708 Hz. The cavities were modeled as sound hard boundary domains, while the metapanel was set with the standard shell physics of the software, in order to reduce computational cost (considering the alternative of using solid mechanics instead). Considering that this procedure shall be used as reference for the DMF and SmEdA methods here analysed, a first stage is to validate it as a reliable source for comparison.

To proceed with the validation, authors choose to investigate a simpler similar model, also investigated by (Maxit *et al.*, 2014): a cavity-plate-cavity system with the same characteristics for the cavities as the ones reported on Section 2. , but with a regular steel plate (mass density $\rho_{plate} = 7800\ kg/m^3$, Young modulus $E_{plate} = 200\ GPa$, damping loss factor $\eta_{plate} = 0.01$) with thickness of 1 mm. Results are shown in Fig. 4a. Results match closely with the cited reference.

Once the reference verified is validated, the cavity-metapanel-cavity system is addressed. The mesh designed to conduct the study can be seen in Fig. 5. It was built considering the rule of a minimum of 6 elements per wavelength, both for the structural boundary (the panel) and the acoustic domains (the cavities).

The structure and the acoustic cavities were discretized by 10632 quad and 55828 hexaedrical elements, respectively. For practicality, authors opt to mirror the panel mesh configuration to the domain. The concentrated masses were added as shell components overlaid with the membrane - also a shell - in order to ensure low computational cost, in spite of requiring the inversion of large matrices for each harmonic frequency.

Once the pressure and velocity of every node is obtained, the total energy associated (kinectic+strain) is calculated for every frequency. A volume integration is conducted for the two cavities, which leads to the obtaining of the Energy Noise Ratio (ENR) as in Eq. 1.

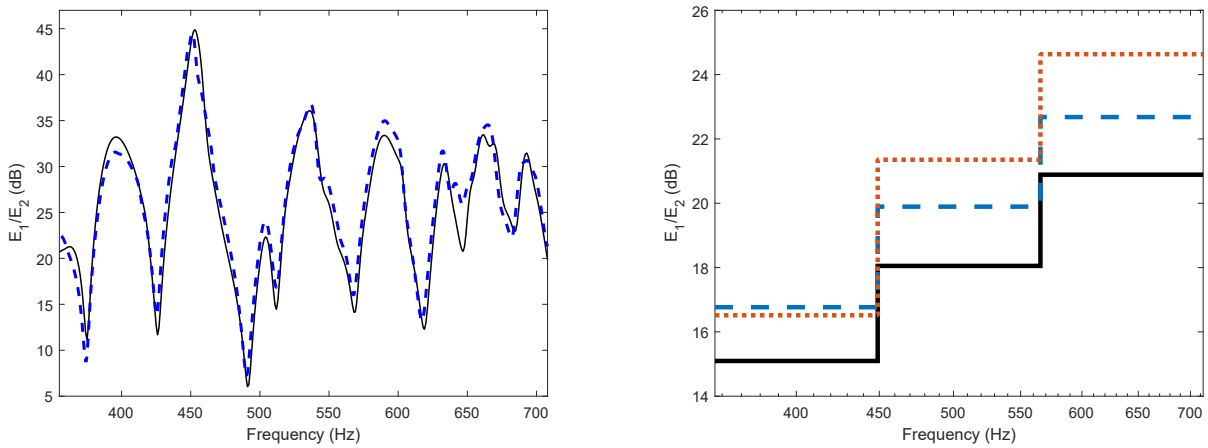

(a) Spectrum (b) Third-octaves average

Figure 4. ENR of the cavity-plate-cavity system. Black solid line, FEM (reference); blue dashed line, DMF; orange dotted line, SmEdA

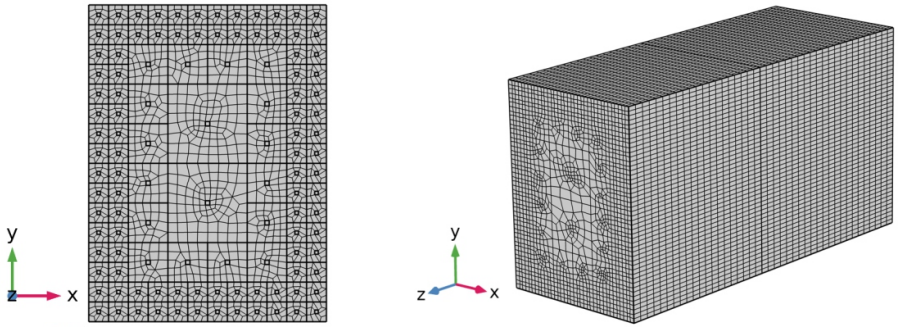

(a) (b)

Figure 5. Vibro-acoustic FEM model (a) front view and (b) angled view.

$$ENR_{(\omega)} = 10\log_{10}\left(\frac{E_1}{E_2}\right) \tag{1}$$

where E_1 and E_2 stands for the total energies of cavities 1 (which contains the monopole source) and 2. TL is then obtained on the range by using Eq. 2.

$$TL_{(\omega)} = ENR - 10log_{10}\left(\frac{V_1}{V_2}\right) - 10log_{10}\left(\frac{4\eta_0\omega V_2}{c_0 S}\right) \tag{2}$$

where S is the area of the panel.

3.2 Modal basis

A relevant part of the diminished computational cost of both the DMF and the SmEdA formulations relies on the fact that the two procedures have as input the modal basis of each uncoupled subsystem involved in the study. Depending on the complexity of the subsystem, analytical strategies can be used to tackle this necessity and produce the modal analyses - as example of what was conducted for a flat simply supported plate in Maxit *et al.* (2014). In the case approached here, as the panel presents some complexity - geometry and material-wise - the modal study of that particular subsystem was conducted on COMSOL FEM environment. The cavities, simple as they are (with straightforward geometry and perfectly rigid walls) were easily handled analytically. Tab. 3 comprises the number of modes calculated for each subsystem on each third-octave band over which the investigation occurs on.

As according to Maxit *et al.* (2014) the non-resonant transmission of structures play a significant role in sound transmission, what are called non-resonant modes are also accounted for the modal basis. A resonant or non-resonant is defined as in Eq. 3, with $\hat{Q}$ representing the modes sets.

Table 3. Number of modes for each third octave band: Nl - number of modes for the excited cavity; Pl^{NR} - number of non-resonant modes for the panel; Pl^{R} - number of resonant modes for the panel; N2 - number of modes for the receiving cavity

	400 Hz	**500 Hz**	**630 Hz**
N1	3	6	14
Pl^{NR}	184	368	606
Pl^{R}	184	238	177
N2	3	6	11

$$\begin{cases} q \in \hat{Q}^{NR} \leftrightarrow \omega_q \in [0, \omega_1[\\ q \in \hat{Q}^{R} \leftrightarrow \omega_q \in [\omega_1, \omega_2] \end{cases} \tag{3}$$

The way in which such data is used as input to the DMF and SmEdA shall be discussed in the next Subsections.

3.3 DMF

Not being a particularly new formulation, the DMF is adequate to portray the dynamic behaviour of a flexible panel coupled with acoustic cavities. DMF is also the basis of SmEdA and a method directly related to SEA. All modelling hereby presented is based on the detailed mathematical process illustrated by Maxit (2013) and Maxit *et al.* (2014). As the scope of the present work does not include the deep description of the methods *per se*, the reader is encouraged to visit the cited references. It is relevant, however, to exhibit Eq. 4, which results from the application of the Fourier transform to the modal equations and shifts the response from time to frequency domain.

$$\begin{bmatrix} Z_{11} & -j\omega W_{12} & 0 \\ j\omega W_{12}^{*} & Z_{22} & j\omega W_{23}^{*} \\ 0 & -j\omega W_{23} & Z_{33} \end{bmatrix} \begin{bmatrix} \Gamma_1 \\ \Gamma_2 \\ \Gamma_3 \end{bmatrix} = \begin{bmatrix} Q_1 \\ 0 \\ 0 \end{bmatrix} \tag{4}$$

in which ω stands for the changing frequency, Z_{11}, Z_{22} and Z_{33} the impedance matrices for the subsystems, W_{12} and W_{23} the modal interaction works matrices, Γ_1, Γ_2 and Γ_3 the modal amplitude vectors for the subsystems and Q_1 the generalised source strength.

The solution to Eq. 4 states the reference for obtaining the averaged energy (in time) of cavity i. The summation of the energy of the subsystems' modes render the total energy of the subsystems, as developed in Maxit and Guyader (2001), assuming the final form as it follows:

$$< E_i >_t = S_{Q_0 Q_0} \int_{\omega_1}^{\omega_2} E_i(\omega) \tag{5}$$

Assuming the system presented in Fig. 2 and detailed in Section 2. the noise transmission from the exciting to the receiving cavity can be defined as in Eq. 6, with $E_1 =< E_1 >_t$ and $E_2 =< E_2 >_t$ being the time-averaged energies of cavities 1 and 2. Eq. 6 relates directly to Eq. 1, but now energies depend on the modal interactions characteristics other than the direct solve of the FEM model. Both ENR and TL are now taken as average over a third-octave band.

$$ENR = 10 \log_{10} \left(\frac{E_1}{E_2} \right) \tag{6}$$

Again, ENR is an input to the classic TL indicator, as Eq. 7 shows.

$$TL = ENR - 10log_{10} \left(\frac{V_1}{V_2} \right) - 10log_{10} \left(\frac{4\eta_0 \omega_c V_2}{c_0 S} \right) \tag{7}$$

where ω_c is the central frequency of the studied third-octave.

3.4 SmEdA

The SmEdA method is capable of describing the energy sharing between the subsystems modes in a given band - generally (and in this work) a third-octave band. Once more the detailed developing of the model will not be presented.

If non-resonant modes are not represented (as they were in DMF), their effect are still considered through the couplings of the two cavities. Here, the structure modes are coupled with the cavities modes by gyroscopic elements, which after all means that "the mass control of the non resonant structure leads to stiffness with the cavity modes" (Maxit *et al.*, 2014). The energy, then, is proportional to the power flow through two gyroscopic oscillators, as Eq. 8 shows.

$$\Pi_{12} = \beta(E_1 - E_2) \tag{8}$$

in which Π_{12} is the time-averaged power flow, E_1 and E_2 the time-averaged energy of the cavities and β a constant depending on the natural angular frequencies and stiffness of the uncoupled oscillators, as well as their damping loss factors and coupling coefficients.

By using, now, β_{pq}, β_{pr} and β_{qr} as modal coupling factors dependent of the interaction modal works W_{pq}, W_{pr} and W_{qr}, a linear equations system of modal energies can be obtained and take into consideration the non-resonant modes:

$$\beta_{pq} = (W_{pq})^2 \frac{(\omega_p \eta_p (\omega_q)^2 + \omega_q \eta_q (\omega_p)^2)}{[(\omega_p)^2 - (\omega_q)^2] + (\omega_p \eta_p + \omega_q \eta_q)[\omega_p \eta_p (\omega_q)^2 + \omega_q \eta_q (\omega_p)^2]} \tag{9}$$

$$\beta_{pr} = \left(\sum_{q \in Q^{NR}} W_{pq} W_{rq} \right)^2 \frac{(\omega_p \eta_p + \omega_r \eta_r)}{[(\omega_p)^2 - (\omega_r)^2] + (\omega_p \eta_p + \omega_r \eta_r)[\omega_p \eta_p (\omega_r)^2 + \omega_r \eta_r (\omega_p)^2]} \tag{10}$$

$$\begin{cases} \omega_p \eta_p E_p + \sum_{q \in \hat{Q}^R} \beta_{pq}(E_p - E_q) + \sum_{r \in \hat{R}} \beta_{pr}(E_p - E_r) = \Pi_{inj}^p, \quad \forall p \in \hat{P} \\ \omega_q \eta_q E_q + \sum_{p \in \hat{P}} \beta_{pq}(E_q - E_p) + \sum_{r \in \hat{R}} \beta_{qr}(E_q - E_r) = 0, \quad \forall q \in \hat{Q}^R \\ \omega_r \eta_r E_r + \sum_{q \in \hat{Q}^R} \beta_{qr}(E_r - E_q) + \sum_{p \in \hat{P}} \beta_{pr}(E_r - E_p) = 0, \quad \forall r \in \hat{R} \end{cases} \tag{11}$$

Lastly, the total energy of each cavity can be obtained by adding all modal energies, like in Eq. 12. The TL, then, can be calculated with the aid of Eq. 6 and Eq. 7.

$$E_1 = \sum_{p \in \hat{P}} E_p, \quad E_2 = \sum_{r \in \hat{R}} E_r \tag{12}$$

4. Results

Initially, COMSOL was used to produce the results with the direct method, by using the model described in Subsection 3.1 with parameters from Tab. 1 for the frequency range comprising the 14^{th}, 15^{th} and 16^{th} third-octaves (355 - 708 Hz). To have a more accurate point of comparison, the numerical procedure for the DMF was also realized by a MATLAB routine, and the two spectrums obtained were plotted overlapped. Figure 6 shows the TL curves formed by the methods.

At a first glance, one can note that the aspect of the two curves is, in parts, similar but shifted in amplitude from each other. That is specially true for the first region of the plot, between 355 and 447 Hz. In terms of modal characteristics, this first third-octave band is strongly dominated by the cavities and comprises a regular dynamics in terms of the panel: there are only mode shapes that happened in plane, and therefore do not affects the TL.

As for the other two third-octaves, the aspect of the curves is very different from each other. A few modes appear with both methods, but other than that, no relation is observed.

To access the general performance of the methods, a more objective indicator is needed. The spectrum is, then, divided into the three third-octaves and the average TL is calculated all for FEM, DMF and SmEda. Results are plotted in Fig. 7 and summarised in Tab. 4.

Table 4. TL (dB) comparison - Third-octave bands

Range (Hz)	**FEM**	**DMF**	**SmEdA**
355-447	23	10.5	15
447-562	20.5	14	17.5
562-708	17	18	20
Octave average	20	14	17.5

The dispersion between methods persist, but diminishes for higher frequencies. DMF and SmEdA show a downwards trend, different than the upwards FEM exhibits. Intuitively, FEM makes the more sense, as third-octave 14 presents high

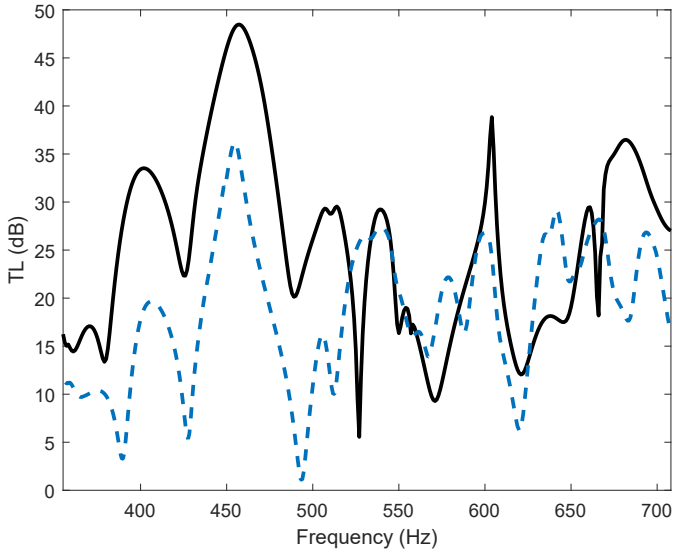

Figure 6. TL of the cavity-panel-cavity system. Black solid line, FEM; blue dashed line, DMF.

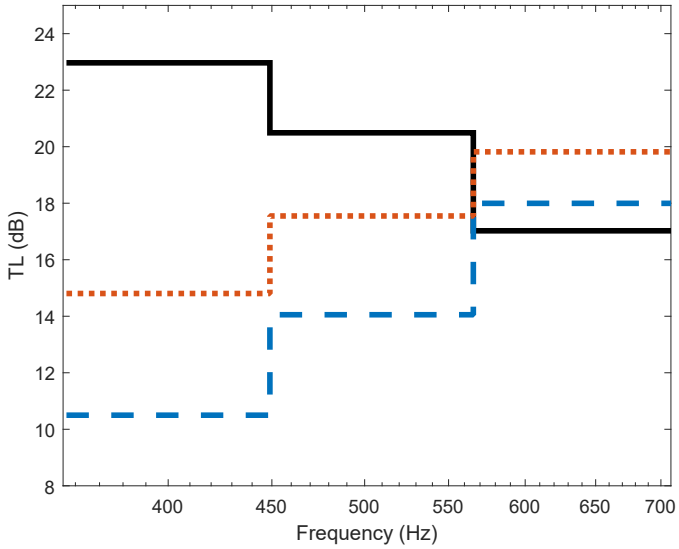

Figure 7. TL of the cavity-panel-cavity system. Black solid line, FEM; blue dashed line, DMF; orange dotted line, SmEdA.

TL because of the mentioned lack of dynamics of the panel; the next region comprises all anti-resonances of the designed cells, while, finally, the last region show lower TL in agreement with the membrane radiating mode of the large cell and downtrend of TL for the two others.

Other than the absolute difference between methods, a relative perspective is in order to allow a more direct view of the error, with respect to FEM results, that the methods presented. Tab. 5 exhibits these deviations, in %.

Table 5. TL (dB) error comparison - Third-octave bands

Range (Hz)	**Err. DMF**	**Err. SmEdA**
355-447	54.3	35.5
447-562	31.4	14.4
562-708	5.7	15.44
Octave average	30.5	16.4

Both methods present a high level of deviation, but if a statement is to be made, SmEdA presents better possibilities on dealing with the complex metapanel. This suggests that the modal basis is insufficient to take into account the energy

transmitted between modes, which could be expected since the modal densisty is low on the investigated frequency range.

The TL performance of the metapanel, which was also assessed in this paper, shows a good prospect, as the subsystem was able to provide 23 dB of attenuation over the aimed frequency range. Considering the ratio TL/mass, with a total mass of 0.245 kg, the panel outperformed the plate previously investigated by far: between 447 and 562 Hz, the plate showed a TL of 23.3 dB, delivering 6.24 dB/kg, in opposition of the 83.6 dB/kg produced by the panel. A remark is made in the sense that this metapanel is, even though a complex system, highly simplified as no holding structure was taken into account. It would decrease the ratio, but at the same time the imposition of mass and new dynamic characteristics should offer a higher TL, summing up to an efficient system.

In terms of computational cost, the direct method took 1 hour and 12 minutes to run, while the obtaining of the modal basis took 28 minutes. DMF and SmEdA ran in 30 seconds. All times relate to the metapanel investigation.

5. CONCLUSIONS

In this paper, the vibro-acoustic behaviour of two rigid closed cavities coupled with a Membrane Acoustic Metamaterial metapanel has been investigated via two distinct numerical modal-based methods: the Dual Modal Formulation and the Statistical Modal Energy Distribution Analysis. With these techniques, the total energy of the cavities was assessed on the low frequency range (in particular, the octave centred at 500 Hz divided into third-octaves intervals) and the Transmission Loss caused by the panel was then obtained.

The numerical routines showed that the modal density in the frequency range in which the analysis occur play an important role on whether the applied method is likely to be successful or not. By comparing the response spectrums with direct FEM results, for example, one can conclude that the modal superposition strategy is not perfectly suitable for the studied range with the given parameters. Let alone, this fact would not be sufficient to affirm the inadequacy of a procedure, as the average result over a range could still converge. The average error of 30.5 % on the octave band leaves also show that the DMF procedure may not be suitable for the targeted problem.

The context is potentially different when considering results reached with SmEdA, but there is not enough data to make a conclusive analysis. The coupling loss factor associated to the subsystems should be experimentally assessed in order to update the models and allow for a more assertive judgement. It would be valuable even to validate the FEM model on a deeper level. In that sense, the superposition of shell physics to form unit cells is yet to be numerically and practically investigated.

As far as the metapanel performance as an acoustic insulator is concerned, the results show the potential of MAM for such applications. Even though the panel has a total mass of approximately 0.245 kg, in opposition to the steel plate of 3.74 kg from Maxit *et al.* (2014), the TL of both systems match up. It is important to highlight that the model suggested here has several simplifications, but it is reasonable to expect that the holding structure of the panel would rise the TL and at the same time be lightweight, resulting in a mass still lower than a conventional panel.

This fact leads directly to the possibility of advancing the investigation reported here by considering a more realistic structure around the panel, in order to comprehend the TL phenomenon in more detailed fashion and, altogether, increase the modal density of the system and enable the usage of DMF and SmEdA and reaching an acceptable level of accuracy. Altogether, other strategies could be taken with the FEM model, such as obtaining the main matrices of the model through COMSOl and running the simulation through MATLAB - as (Maxit, 2013) successfully performed. Another step posterior works could comprehend is to vary the coupling loss factor from the subsystems, in order to acquire more repertoire over the transmission phenomenon.

6. ACKNOWLEDGEMENTS

The authors acknowledge the financial support of the São Paulo State Research Foundation (FAPESP) under grant # 2018/15894-0. They also thank the National Council for the Improvement of Higher Education - CAPES for the scholarship awarded to the first author (grant # 88887.498369/2020-00).

7. REFERENCES

Aloufi, B., Behdinan, K. and Zu, J., 2016. "Theoretical vibro-acoustic modeling of acoustic noise transmission through aircraft windows". *Journal of Sound Vibration*, Vol. 371, pp. 344–369. doi:10.1016/j.jsv.2016.02.023.

Aridogan, U. and Basdogan, I., 2015. "A review of active vibration and noise suppression of plate-like structures with piezoelectric transducers". *Journal of Intelligent Material Systems and Structures*, Vol. 26. doi: 10.1177/1045389X15585896.

Bragg, W.H. and Bragg, W.L., 1913. "The reflection of X-rays by crystals". *Proceedings of the Royal Society of London. Series A, Containing Papers of a Mathematical and Physical Character*, Vol. 88, No. 605, pp. 428–438.

Chen, Y., Huang, G., Zhou, X., Hu, G. and Sun, C.T., 2014. "Analytical coupled vibroacoustic modeling of membrane-type acoustic metamaterials: Plate model". *The Journal of the Acoustical Society of America*, Vol. 136, No. 6, pp.

2926–2934.

Fan, L., Chen, Z., Zhang, S.y., Ding, J., Li, X.j. and Zhang, H., 2015. "An acoustic metamaterial composed of multi-layer membrane-coated perforated plates for low-frequency sound insulation". *Applied Physics Letters*, Vol. 106, No. 15.

Guy, R.W., 1979. "The response of a cavity backed panel to external airborne excitation: A general analysis". *The Journal of the Acoustical Society of America*, Vol. 65, No. 3, pp. 719–731. doi:10.1121/1.382485. URL https://doi.org/10.1121/1.382485.

Hong, K. and Kim, J., 1995. "Analysis of free vibration of structural-acoustic coupled systems .2. two- and three-dimensional examples". *Journal of Sound and Vibration*, Vol. 188, pp. 577–600. doi:10.1006/jsvi.1995.0612.

Langfeldt, F., Gleine, W. and von Estorff, O., 2018. "An efficient analytical model for baffled, multi-celled membrane-type acoustic metamaterial panels". *Journal of Sound and Vibration*, Vol. 417, pp. 359–375.

Ma, F., Wang, C., Liu, C. and Wu, J.H., 2021. "Structural designs, principles, and applications of thin-walled membrane and plate-type acoustic/elastic metamaterials". *Journal of Applied Physics*, Vol. 129, No. 23, p. 231103. doi:10.1063/5.0042132. URL https://doi.org/10.1063/5.0042132.

Martin, P., 2015. "Advanced computational vibroacoustics: Reduced-order models and uncertainty quantification". *The Journal of the Acoustical Society of America*, Vol. 137, pp. 2182–2182. doi:10.1121/1.4914994.

Maxit, L., Ege, K., Totaro, N. and Guyader, J., 2014. "Non resonant transmission modelling with statistical modal energy distribution analysis". *Journal of Sound and Vibration*, Vol. 333, No. 2, pp. 499–519. ISSN 0022-460X. doi:https://doi.org/10.1016/j.jsv.2013.09.007. URL https://www.sciencedirect.com/science/article/pii/S0022460X13007414.

Maxit, L. and Guyader, J.L., 2001. "Estimation of sea coupling loss factors using a dual formulation and fem modal information, part i: Theory". *Journal of Sound and Vibration*, Vol. 239, No. 5, pp. 907–930. ISSN 0022-460X. doi:https://doi.org/10.1006/jsvi.2000.3192. URL https://www.sciencedirect.com/science/article/pii/S0022460X00931924.

Maxit, L., 2013. "Analysis of the modal energy distribution of an excited vibrating panel coupled with a heavy fluid cavity by a dual modal formulation". *Journal of Sound and Vibration*, Vol. 332, No. 25, pp. 6703–6724. ISSN 0022-460X. doi:https://doi.org/10.1016/j.jsv.2013.07.020. URL https://www.sciencedirect.com/science/article/pii/S0022460X13006342.

Möser, M. and Zimmermann, S., 2004. *Engineering Acoustics: An Introduction to Noise Control*. Engineering online library. Springer. ISBN 9783540202363. URL https://books.google.com.br/books?id=JN9gQXGqdOQC.

Mosquera-Sánchez, J., Sarrazin, M., Janssens, K., de Oliveira, L. and Desmet, W., 2018. "Multiple target sound quality balance for hybrid electric powertrain noise". *Mechanical Systems and Signal Processing*, Vol. 99, pp. 478–503. doi:10.1016/j.ymssp.2017.06.034. URL https://doi.org/10.1016/j.ymssp.2017.06.034.

Mosquera-Sánchez, J.A., Desmet, W. and de Oliveira, L.P., 2017a. "A multichannel amplitude and relative-phase controller for active sound quality control". *Mechanical Systems and Signal Processing*, Vol. 88, pp. 145–165. doi:10.1016/j.ymssp.2016.10.036. URL https://doi.org/10.1016/j.ymssp.2016.10.036.

Mosquera-Sánchez, J.A., Desmet, W. and de Oliveira, L.P., 2017b. "Multichannel feedforward control schemes with coupling compensation for active sound profiling". *Journal of Sound and Vibration*, Vol. 396, pp. 1–29. doi:10.1016/j.jsv.2017.02.016. URL https://doi.org/10.1016/j.jsv.2017.02.016.

Nguyen, H., Wu, Q., Chen, J., Yu, Y., Chen, H., Tracy, S. and Huang, G., 2021. "A broadband acoustic panel based on double-layer membrane-type metamaterials". *Applied Physics Letters*, Vol. 118, No. 18, p. 184101. doi:10.1063/5.0042584. URL https://doi.org/10.1063/5.004258.

Pan, J. and Bies, D.A., 1990. "The effect of fluid–structural coupling on sound waves in an enclosure—theoretical part". *The Journal of the Acoustical Society of America*, Vol. 87, No. 2, pp. 691–707. doi:10.1121/1.398939. URL https://doi.org/10.1121/1.398939.

Ruiz, A.G., Santos, J.C., Croes, J., Desmet, W. and da Silva, M.M., 2018. "On redundancy resolution and energy consumption of kinematically redundant planar parallel manipulators". *Robotica*, Vol. 36, No. 6, pp. 809–821. doi:10.1017/s026357471800005x. URL https://doi.org/10.1017/s026357471800005x.

Sampaio, L.Y.M., Cerântola, P.C.M. and de Oliveira, L.P.R., 2019. "Lightweight decorated membrane panels for sound isolation". In *Proceedings of ISMA2020 - International Conference on Noise and Vibration Engineering*. Leuven, Belgium, pp. 545–558.

Sandberg, G. and Ohayon, R., 2009. *Computational aspects of structural acoustics and vibration*, Vol. 505. Springer Science & Business Media.

Venter, G.S., do Paraizo Silva, L.M., Carneiro, M.B. and da Silva, M.M., 2016. "Passive and active strategies using embedded piezoelectric layers to improve the stability limit in turning/boring operations". *The International Journal of Advanced Manufacturing Technology*, Vol. 89, No. 9-12, pp. 2789–2801. doi:10.1007/s00170-016-9620-2. URL https://doi.org/10.1007/s00170-016-9620-2.

Yang, Z., Mei, J., Yang, M., Chan, N. and Sheng, P., 2008. "Membrane-type acoustic metamaterial with negative dynamic mass". *Physical review letters*, Vol. 101, No. 20.

8. RESPONSIBILITY NOTICE

The authors are solely responsible for the printed material included in this paper.